Coupled Mode Theory of Parallel Waveguides

AMOS HARDY SENIOR MEMBER, IEEE, AND WILLIAM STREIFER FELLOW, IEEE

Abstract—A new coupled mode formulation for parallel dielectric waveguides is described. The results apply to any guided modes (TE, TM, or hybrid) in waveguides of arbitrary cross-section, dissimilar index, and nonidentical shape. Additional index perturbations not included within the waveguides are encompassed by the theory. Propagation constants and mode patterns for the coupled modes computed according to this theory are shown to agree very well with numerical solutions for the system modes when the latter can be determined. Moreover, the new results are more accurate than those obtained from prior coupled mode formulations. It is shown that even for lossless guides the coupling coefficients from waveguide "b" to "a" and from "a" to "b," described by κ_{ab} and κ_{ba}, respectively, are not related by their complex conjugates if the guides are not identical.

I. Introduction

COUPLING BETWEEN parallel waveguides has long been a subject of interest in the fields of integrated optics [1]–[4] and semiconductor diode lasers [5]–[9]. Even today in the integrated optics area researchers are concerned with the topic in applications relating to modulators, switches, and signal processing whereas in the diode laser field, scanning, longitudinal mode control, and phased arrays involve coupling situations. But in spite of the substantial interest in the coupling problem, little progress has been made in understanding the process. Most analyses still employ the coupled mode formulations developed by Marcuse [10], Yariv [11], and Taylor and Yariv [4]. Their results, even though intended for arbitrary waveguides, are accurate only in special cases of near identical waveguides in weak coupling situations. Difficulties with the prior theory have been recognized by various researchers. Specifically, Suematsu and Kishino [12] attacked the problem by using a method based on the interference between the modes of the coupled system while Marom *et al.* [13] discussed some of the shortcomings in the formulation but did not resolve them. Fundamentally, the difficulties with coupled mode theory arise because the interaction of the individual waveguide modes are inadequately described by the prior theory even in the case of weak coupling as shown below in this paper. Although coupled mode theory utilizes the interaction of the individual waveguide modes, and is thereby inherently limited, it is possible to develop the theory in a self-consistent manner by retaining the radiation modes in the derivation and neglecting them only after their influence is determined. In this way we obtain unambiguous formulas for propagation constants and coupling coefficients which are more accurate than those previously published. The increased accuracy is particularly significant for coupling between nonidentical waveguides. It is evident even for weak coupling and the new formulation appears to extend coupled mode theory to more strongly coupled waveguide geometries; it becomes inaccurate in the very strong coupling limit.

Prior to discussing our results it is worthwhile to review some conclusions of previous theories. For coupling between identical waveguides the results are quite straightforward in that κ_{ab}, the coupling coefficient from guide "b" to guide "a," is identical to κ_{ba}, whether or not the system contains loss or gain. For nonidentical waveguides the situation is more complicated. First, one reads that even though the waveguides differ, when neither loss nor gain are present, κ_{ab} and κ_{ba} are related by their complex conjugates [4], [10]. Although this result is represented as following from power conservation considerations, it is incorrect because the expression for power flow ignores cross terms between the two waveguide fields. The cross terms depend upon the integrated overlap of the individual waveguide modes over all space. Thus these integrals are substantially larger than those appearing in the traditional coupling coefficient definitions which contain integrations of the overlapping fields only in the waveguides themselves. Furthermore, even in the lossless case the expressions for κ_{ab} and κ_{ba} differ for nonidentical waveguides. One of these contains $\Delta\epsilon^{(a)}$ and the other $\Delta\epsilon^{(b)}$, where these functions are the perturbations to waveguides "a" and "b" respectively. But for nonidentical waveguides, $\Delta\epsilon^{(a)}$ and $\Delta\epsilon^{(b)}$ differ as do the numerically computed values of κ_{ab} and κ_{ba}. Consequently, according to the defining equations, the coupling coefficients are not complex conjugates even for lossless waveguides. Still another difficulty concerns the definitions of κ_{ab} and κ_{ba} themselves for nonidentical coupled waveguides. If we refer to [10] or complete the derivation of [4], which is specialized in that reference for the case of identical waveguides, we find that the integral for κ_{ab} contains $\Delta\epsilon^{(b)}$ and κ_{ba} depends analogously on $\Delta\epsilon^{(a)}$; however, in [14] the definitions are exactly reversed and therefore yield contradictory results for nonidentical waveguides. The difficulty with the derivation of [4], [10] is that the modes of the two individual waveguides are implicitly assumed orthogonal. Rather, as we have noted above in connection with the power flow, the modal overlap integral is large, not small, compared to the integral appearing in the coupling coefficient. Thus

Manuscript received January 23, 1985; revised April 17, 1985 and June 5, 1985.

A. Hardy was with Xerox Palo Alto Research Center, Palo Alto, CA 94304, on leave from the Faculty of Engineering, Tel Aviv University, Tel Aviv, Israel.

W. Streifer was with Xerox Palo Alto Research Center, Palo Alto, CA. He is now with the Center for High Technology Materials, University of New Mexico, Albuquerque, NM 87131.

0733-8724/85/1000-1135$1.00

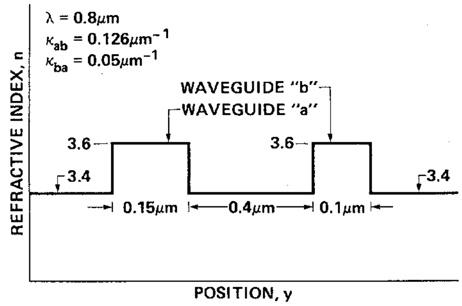

Fig. 1. Illustrating the coupling between dissimilar waveguides in which the guided mode of waveguide "b" couples efficiently into waveguide "a," but not conversely, i.e., $|\kappa_{ab}|^2 \gg |\kappa_{ba}|^2$. Power is conserved in this process.

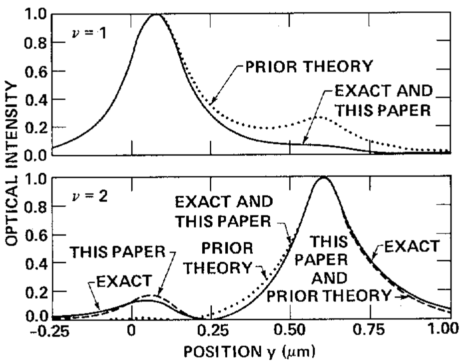

Fig. 2. Intensities of the $\nu = 1$ and $\nu = 2$ array modes in the geometry of Fig. 1. Note that for $\nu = 2$ the dotted curve calculated according to the prior theory is approximately coincident with the axis in the vicinity of $y = 0$.

the overlap is a first order not a second order effect or perturbation. Moreover, disregarding the effect of radiation fields early in the derivation is an additional source of error. The development of [14] on the other hand is related to our own, but there the early neglect of the radiation fields and the assumed array mode form introduce even more severe errors. Thus although some of our expressions resemble those of [14], our calculated coefficients agree qualitatively with [10] and the completed derivation of [4] rather than [14].

To illustrate the new theory, consider the two parallel planar optical waveguides depicted in Fig. 1. The dimensions and refractive indexes are such that only one TE mode propagates in each guide individually. With $\lambda = 0.8$ μm, a numerical solution for the two array modes of the two-waveguide system yields propagation constants $\sigma_1 = 27.201$ μm^{-1} and $\sigma_2 = 26.931$ μm^{-1}, which compare favorably with the results of this paper, i.e., $\sigma_1 = 27.200$ μm^{-1} and $\sigma_2 = 26.926$ μm^{-1}. According to the prior theory $\sigma_1 = 27.210$ μm^{-1} and $\sigma_2 = 26.953$ μm^{-1}. Thus the beat length between the two array modes, i.e., $2\pi/(\sigma_1 - \sigma_2)$, as calculated by our theory, differs from the exact value by ≈ 1.5 percent, whereas the prior results are inaccurate by ≈ 5 percent. In Fig. 2(a) and (b) we display intensity patterns for the array modes computed as above. For the $\nu = 1$ mode, i.e., σ_1, the exact intensity pattern and that computed by the theory of this paper are undistinguishable in Fig. 2(a). Slight differences are evident for the $\nu = 2$ mode in Fig. 2(b), but the accuracy of the new theory for both propagation constants and mode patterns strongly encourages us to have confidence in the new formulation.

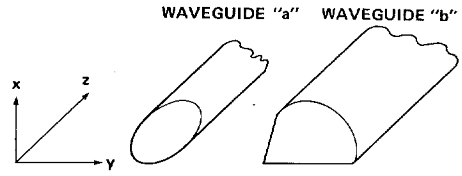

Fig. 3. Schematic of two parallel optical waveguides.

Our calculations also show that $|\kappa_{ab}|$ exceeds $|\kappa_{ba}|$ by a factor of ≈ 2.5 at $\lambda = 0.8$ μm (see Fig. 1). Physically we observe that waveguide "b" is a much weaker guide than "a" as a result of its lesser thickness. Thus the individual guided mode propagating in "b" extends influentially into waveguide "a" and couples strongly into the guided mode of "a." In contrast, the mode "a" is relatively well confined and is weak in the vicinity of guide "b," cf., Fig. 2(a). Hence it does not couple effectively into mode "b." Nevertheless, numerical calculations indicate that the net power transfer between lossless nonidentical waveguides is symmetrical as required by reciprocity.

In addition to the results described above, the theory developed in this paper applies generally to parallel optical waveguides of arbitrary cross-section, dissimilar index, and nonidentical shape for all guided mode types, i.e., TE, TM, and hybrid. Accurate formulas are derived for the propagation constants and coupling coefficients. Moreover, the presence of index perturbations external to the waveguides are included in the formulas.

Section II of this paper outlines briefly the coupled mode formulation. Power flow and power transfer between the coupled guides is discussed in Section III. Examples of coupling between parallel slab waveguides are presented in Section IV and the results are summarized in Section V. The paper concludes with several mathematical appendixes.

II. The Coupled Mode Equations

The formulation developed in this section is based in part on the general coupled mode theory for one perturbed waveguide as expounded by Kogelnik [15]. His notation is employed, whenever convenient, with the notable exception of the time dependence. We use $\exp(-i\omega t)$ so that propagation in the $+z$ direction is described by $\exp(i\beta z)$; corresponding equations may be compared by replacing consistently $-j$ in [15] by $+i$. Moreover, our treatment is generalized to include complex refractive indexes and fields. Consider now two parallel dielectric waveguides denoted "a" and "b," which may differ in shape, size, and/or refractive index (see Fig. 3). If the refractive indexes are real, then clearly the waveguide index must exceed that of the surroundings.

The modal vectorial fields of the individual guides are designated by superscripts (a) and (b), respectively. Now following Kogelnik [15], we consider an electromagnetic field $\{E(x, y, z), H(x, y, z)\}$ which satisfies Maxwell's equations plus the boundary conditions of the entire structure, as is shown in Fig. 3. Such fields include the guided modes of the entire waveguide structure. For this discussion we assume that each individual waveguide supports only one guided mode so that the transverse field may be written

$$\boldsymbol{E}_t(x, y, z) = U(z)\, \boldsymbol{E}_t^{(a)}(x, y) + V(z)\, \boldsymbol{E}_t^{(b)}(x, y) + \boldsymbol{E}_r(x, y, z) \tag{1a}$$

and

$$\boldsymbol{H}_t(x, y, z) = U(z)\, \boldsymbol{H}_t^{(a)}(x, y) + V(z)\, \boldsymbol{H}_t^{(b)}(x, y) + \boldsymbol{H}_r(x, y, z) \tag{1b}$$

where $U(z)$ and $V(z)$ express the z-dependence of the individual guided modes whose transverse fields are $\{\boldsymbol{E}_t^{(a)}, \boldsymbol{H}_t^{(a)}\}$, $\{\boldsymbol{E}_t^{(b)}, \boldsymbol{H}_t^{(b)}\}$, and $\boldsymbol{E}_r$ and $\boldsymbol{H}_r$ are the residual fields. Since the system modes are not exactly linear combinations of the individual waveguide modes, $\boldsymbol{E}_r$ and $\boldsymbol{H}_r$ are required for these to be equations. In our derivation we demand that the residue field be orthogonal to both $\boldsymbol{E}_t^{(a)}$ and $\boldsymbol{E}_t^{(b)}$, and that requirement leads to the more accurate expressions derived herein. The residue field may or may not be completely guided by the system of two waveguides depending on whether or not $\{\boldsymbol{E}_t, \boldsymbol{H}_t\}$ is a guided mode of the system. In both cases the residue field is expressed formally in terms of the radiation modes of either waveguide, but it is unnecessary to calculate it explicitly. Generally, our interest is limited to geometries in which the modal fields of the entire structure are well represented by a superposition of the fundamental individual waveguide modes so that the fields $\{\boldsymbol{E}_t, \boldsymbol{H}_t\}$ under consideration are those for which $\boldsymbol{E}_r$ (and $\boldsymbol{H}_r$) are small in comparison with the other terms. But the full forms of $\boldsymbol{E}_t$ and $\boldsymbol{H}_t$ as represented in (1a) and (1b) are retained throughout the derivation, and $\boldsymbol{E}_r$, $\boldsymbol{H}_r$ are neglected only at its conclusion.

Our objective is to derive differential equations relating $U(z)$ and $V(z)$. The derivation is quite mathematical and tedious; it appears in its entirety in Appendix B. Following substantial manipulation, we obtain

$$\frac{dU}{dz} = i\gamma^{(a)}U + i\kappa_{ab}V \tag{2a}$$

$$\frac{dV}{dz} = i\gamma^{(b)}V + i\kappa_{ba}U \tag{2b}$$

where the effects of the residual fields have been neglected only after deriving expressions for the coefficients in (2a) and (2b). The propagation constants $\gamma^{(a)}$ and $\gamma^{(b)}$ are given by

$$\gamma^{(a)} = \beta^{(a)} + [\tilde{\kappa}_{aa} - C_{ab}\tilde{\kappa}_{ba} + C_{ab}C_{ba}(\beta^{(a)} - \beta^{(b)})]/(1 - C_{ab}C_{ba}) \tag{3a}$$

and

$$\gamma^{(b)} = \beta^{(b)} + [\tilde{\kappa}_{bb} - C_{ba}\tilde{\kappa}_{ab} + C_{ab}C_{ba}(\beta^{(b)} - \beta^{(a)})]/(1 - C_{ab}C_{ba}) \tag{3b}$$

where the corrections to the individual waveguide mode propagation constants $\beta^{(a)}$ and $\beta^{(b)}$ describe the effects of the modal interactions. The coupling coefficients are

$$\kappa_{ab} = \{\tilde{\kappa}_{ab} + C_{ab}[\beta^{(a)} - \beta^{(b)} - \tilde{\kappa}_{bb}]\}/(1 - C_{ab}C_{ba}) \tag{4a}$$

and

$$\kappa_{ba} = \{\tilde{\kappa}_{ba} + C_{ba}[\beta^{(b)} - \beta^{(a)} - \tilde{\kappa}_{aa}]\}/(1 - C_{ab}C_{ba}). \tag{4b}$$

In (3a)–(4b), the coefficients C_{ab} and C_{ba} describe the individual waveguide mode overlap, i.e.,

$$C_{pq} = 2\hat{z} \cdot \iint_{-\infty}^{\infty} [\boldsymbol{E}_t^{(q)} \times \boldsymbol{H}_t^{(p)}]\, dx\, dy, \qquad p, q = a, b \tag{5}$$

and we anticipate that C_{pq} will appear in power flow equations describing the joint interactions of the individual waveguide modes. The individual modes are normalized (see Appendix A) such that

$$C_{aa} = C_{bb} = 1. \tag{6}$$

The constants $\tilde{\kappa}_{pq}$ depend on the perturbations to the individual waveguides and are defined by

$$\tilde{\kappa}_{pq} = \omega \iint_{-\infty}^{\infty} \Delta\epsilon^{(p)}\left[\boldsymbol{E}_t^{(p)} \cdot \boldsymbol{E}_t^{(q)} - \frac{\epsilon^{(q)}}{\epsilon_0 n^2} E_z^{(p)}E_z^{(q)}\right] dx\, dy, \qquad p, q = a, b \tag{7}$$

where $\epsilon^{(p)}$, $p = a, b$ refer to the individual waveguides and $\Delta\epsilon^{(p)}$, $p = a, b$ are the perturbations to the respective guide. Note that the integrals in (7) extend only over the regions in which the perturbations occur. For example, in a simple case, waveguide "b" is the perturbation to waveguide "a," and conversely. In contrast, the integrals in (5) extend over all space.

More complicated waveguiding structures are decomposed into two individual guides as follows

$$\epsilon^{(a)}(x, y) + \Delta\epsilon^{(a)}(x, y) = \epsilon_0 n^2(x, y) \tag{8a}$$

and

$$\epsilon^{(b)}(x, y) + \Delta\epsilon^{(b)}(x, y) = \epsilon_0 n^2(x, y) \tag{8b}$$

where $\epsilon^{(a)}(x, y)$ and $\epsilon^{(b)}(x, y)$ each represent the individual waveguides singly embedded in the surrounding medium. Note that $\epsilon^{(a)}(x, y) + \epsilon^{(b)}(x, y) \neq \epsilon(x, y) = \epsilon_0 n^2(x, y)$, since each function contains the same surroundings. Moreover, most generally $\epsilon_0 n^2(x, y)$ need not even equal the mathematical union of $\epsilon^{(a)}(x, y)$ and $\epsilon^{(b)}(x, y)$, because an additional index perturbation not encompassed by either waveguide could be included.

In [4], quantities labeled $M_{(a)}$ and $M_{(b)}$ were derived (see [4, eq. (52)]) as corrections to the propagation constants, i.e., $\gamma^{(p)} = \beta_1^{(p)} - iM_{(p)}$, $p = a, b$. The expressions for

$M_{(p)}$, aside from the multiplicative factor $-i$, differ from $\tilde{\kappa}_{pp}$ in that the latter include integrals which contain the z-components of the individual waveguide modes. Those integrals vanish for TE modes, but even then (3a) and (3b) for $\gamma^{(p)}$, $p = a, b$, are more accurate in that they incorporate $\tilde{\kappa}_{ab}$, $\tilde{\kappa}_{ba}$, C_{ab}, and C_{ba}. An expression for the coupling coefficient κ_{ab} is also derived in [4] but is immediately specialized to the case of identical waveguides. Completing the derivation of [4] for dissimilar waveguides yields

$$\bar{\kappa}_{ab} = \omega \iint_{-\infty}^{\infty} \Delta\epsilon^{(b)} \boldsymbol{E}_{t_1}^{(a)} \cdot \boldsymbol{E}_{t_1}^{(b)} \, dx\, dy \tag{9a}$$

and

$$\bar{\kappa}_{ba} = \omega \iint_{-\infty}^{\infty} \Delta\epsilon^{(a)} \boldsymbol{E}_{t_1}^{(b)} \cdot \boldsymbol{E}_{t_1}^{(a)} \, dx\, dy. \tag{9b}$$

(although one finds $\Delta\epsilon^{(a)}$ and $\Delta\epsilon^{(b)}$ reversed occasionally in the literature [14]). Thus $\bar{\kappa}_{ba}$ resembles $\tilde{\kappa}_{ab}$ in (7) without the second integral and similarly for $\bar{\kappa}_{ab}$ and $\tilde{\kappa}_{ba}$; however, as demonstrated in Section IV, although κ_{ab} and $\bar{\kappa}_{ab}$ do not have similar forms, the latter does approximate the former numerically just as $\bar{\kappa}_{ba}$ approximates κ_{ba}.

It is important to note that neither κ_{ab} and κ_{ba} as defined by (4a) and (4b) nor $\bar{\kappa}_{ab}$ and $\bar{\kappa}_{ba}$ in (9a) and (9b) satisfy complex conjugate relationships for lossless waveguides unless the guides are identical. The usual derivation of that result relies on an approximate application of power conservation and is discussed in greater detail in Section III.

III. Power Flow and Power Transfer Between Parallel Waveguides

The time averaged power flow in the z-direction is given by

$$P_z = \tfrac{1}{2}\hat{z} \cdot \iint_{-\infty}^{\infty} \mathrm{Re}\,(\boldsymbol{E}_t \times \boldsymbol{H}_t^*)\, dx\, dy. \tag{10}$$

Now if the unperturbed waveguide system has neither loss nor gain (hereafter referred to as lossless) then we obtain

$$P_z = \tfrac{1}{4}[|U|^2 + |V|^2 + (C_{ab} + C_{ba})\,\mathrm{Re}\,(UV^*)] + \tfrac{1}{2}\hat{z} \cdot \iint_{-\infty}^{\infty} \mathrm{Re}\,(\boldsymbol{E}_r \times \boldsymbol{H}_r^*)\, dx\, dy \tag{11}$$

upon substituting (1a) and (1b) in (10). The usual derivations showing that $\kappa_{ab} \equiv \kappa_{ba}^*$ in a lossless system employs only the first two terms of (11). In the following discussion only the last term is neglected.

Let us consider two parallel lossless guides with $U \equiv 0$ and $V = V_0$ at $z = 0$. We do not address the question of how that initial connection is established, but that issue must be considered in any analysis regardless of the equations used to describe the propagation and coupling along the length where the guides are parallel. Upon solving (2a) and (2b) subject to these initial conditions, we obtain

$$V(z) = V_0 \left[\cos(\psi z) + \frac{i\Delta}{\psi}\sin(\psi z)\right] e^{i\phi z} \tag{12a}$$

and

$$U(z) = V_0 \frac{i\kappa_{ab}}{\psi} \sin(\psi z)\, e^{i\phi z} \tag{12b}$$

where

$$\phi = [\gamma^{(a)} + \gamma^{(b)}]/2 \tag{13a}$$

$$\Delta = [\gamma^{(b)} - \gamma^{(a)}]/2 \tag{13b}$$

and

$$\psi = \sqrt{\Delta^2 + \kappa_{ab}\kappa_{ba}} \tag{13c}$$

We observe that when $\psi z = \pi/2$, $|U|$ is a maximum. If waveguide "b" could be terminated at that point, the modal amplitude and power in "a" can be estimated. We multiply the entire field by $\boldsymbol{H}_t^{(a)}$ and integrate to obtain $U + C_{ab}V$. Based on this estimate the power remaining in waveguide "a" is given by

$$P^{(a)} = \frac{1}{4}|U + C_{ab}V|^2 = \frac{1}{4}\frac{|V_0|^2}{\psi^2}|\kappa_{ab} + C_{ab}\Delta|^2 \tag{14}$$

and this result is independent of the formula used to evaluate κ_{ab}.

Instead, however, let the coupling process begin with $U = V_0$ and $V = 0$ at $z = 0$. If after propagating $\psi z = \pi/2$, waveguide "a" can be terminated, then as above the modal amplitude in waveguide "b" would be $V + C_{ba}U$. Consequently, the power remaining in waveguide "b" is estimated to be

$$P^{(b)} = \frac{1}{4}|V + C_{ba}U|^2 = \frac{1}{4}\frac{|V_0|^2}{\psi^2}|\kappa_{ba} - C_{ba}\Delta|^2. \tag{15}$$

In order to satisfy reciprocity in a lossless waveguide system, $P^{(a)}$ and $P^{(b)}$ as given by (14) and (15) should be equal. We cannot demonstrate that result analytically and indeed it cannot be exactly true because the residue fields have been neglected. However, we show numerically late in Section IV that $P^{(a)}$ and $P^{(b)}$ in (14) and (15) differ negligibly.

Finally, in order that power be conserved when propagating along z, P_z must be independent of z. Equations (12a) and (12b) are substituted in (11), with the residue fields neglected, to obtain

$$P_z = \frac{1}{4}|V_0|^2\left\{1 + \frac{\kappa_{ab}}{\psi^2}[(\kappa_{ab} - \kappa_{ba}) + \Delta(C_{ab} + C_{ba})]\sin^2(\psi z)\right\}. \tag{16}$$

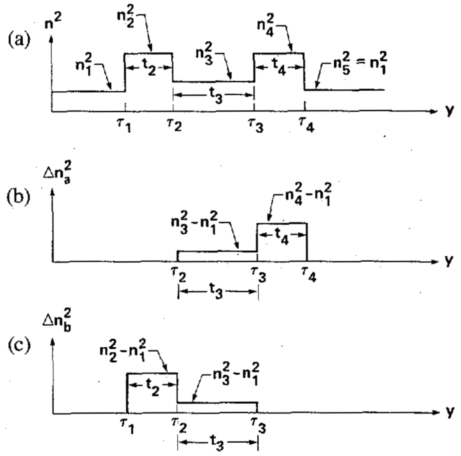

Fig. 4. (a) (b) (c) Two planar guides with an index perturbation of the inner region.

Now for P_z = constant, the coefficient of the $\sin^2(\psi z)$ term must be zero, but except for identical guides we cannot demonstrate that result analytically. This deficiency should be expected since the last term of (11) has been neglected and the equality in the case of identical guides is only fortuitous. Nevertheless, for a large number of examples of TE modes in slab waveguides, including the geometry of Fig. 1, in which κ_{ab} and κ_{ba} differ greatly, the discrepancy represented by the $\sin^2 \psi z$ term of (16) has never exceeded a very small fraction of a percent. The discrepancy is much greater if only the $|U|^2$ and $|V|^2$ terms are included in P_z and the values of $\bar{\kappa}_{ab}$ and $\bar{\kappa}_{ba}$ are used in the calculation. Examples illustrating the magnitude of the $\sin^2 \psi z$ term in (16) are discussed in the concluding paragraphs of the next section.

IV. Examples

In this section we calculate propagation constants and coupling coefficients for TE modes (see Appendix C) of the two coupled slab waveguides illustrated in Fig. 4(a). The functions Δn_a^2 and Δn_b^2 are illustrated in Fig. 4(b) and (c). All refractive indexes are assumed real except in the region between the guides where n_3^2 is taken to be complex, thereby representing the presence of optical loss or gain. The individual waveguides in such a structure usually support only a single TE mode (in practical cases). The system modes are computed by solving numerically the scalar wave equation of the entire system and the resulting eigenvalue equation. That process is somewhat complicated when the refractive indices are complex. Alternatively, one may neglect initially the imaginary part of n_3^2 and solve for the real propagation constants and the mode patterns. Next, the fraction of modal power confined to region 3 is determined, i.e., the "filling factor," and the real propagation constants are perturbed by the loss or gain weighted by the filling factor to yield σ_1 and σ_2. For the gain or loss values considered here, the perturbation to the real part of the propagation constant is on the order of 1 part in 10^{10} and in this section we take σ_1 and σ_2, determined by this method to be the "exact" results against which the coupled mode results are compared.

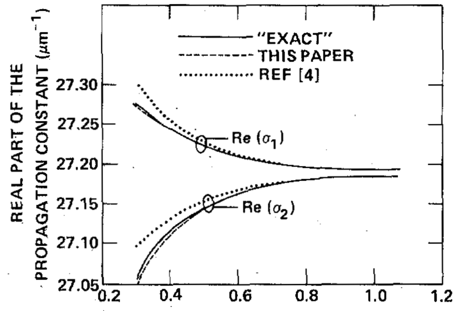

(a)

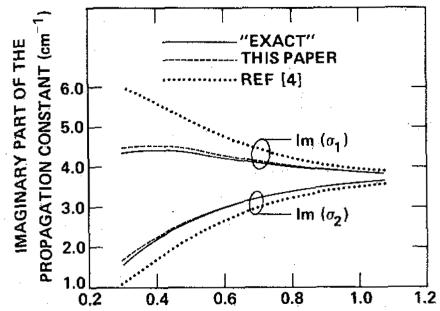

(b)

Fig. 5. (a) (b) Propagation constants versus thickness of region 3 for identical waveguides.

As an initial example, the individual waveguides are presumed identical with $n_1 = n_5 = \text{Re}(n_3) = 3.4$ and $n_2 = n_4 = 3.6$. The waveguide thicknesses are $t_2 = t_4 = 0.15$ μm, the wavelength is $\lambda = 0.8$ μm, and the additional power loss or gain between the guides in region 3 is 30 cm^{-1}, i.e., $\Delta n_3^2 = \pm i\, 1.299 \times 10^{-3}$, where the positive sign corresponds to material loss. Results for the symmetric TE mode σ_1, and the antisymmetric TE mode σ_2, as a function of the guide separation t_3 are plotted in Fig. 5. In Fig. 5(a) we display Re (σ_1) and Re (σ_2) where the solid curves labeled "exact" were calculated as described immediately above. The dashed curves were obtained by adding $\Delta n_c^2 = \text{Im}(n_3^2)$ integrated over t_3 to $\Delta n_a^2 = n_4^2 - n_1^2$, as shown in Fig. 4(b). Similarly, $\Delta n_c^2 = \text{Im}(n_3^2)$ and $\Delta n_b^2 = n_2^2 - n_1^2$ are both shown in Fig. 4(c), but as noted above Im (n_3^2) has a negligible effect on Re (σ_1) and Re (σ_2). Finally, the dotted curves were determined from the equations of [4], which for the TE modes with $\beta_1^{(a)} = \beta_1^{(b)}$ simply follow from our formulation by setting $C_{ab} = C_{ba} = 0$. The same conventions are employed in Fig. 5(b), where Im (σ_1) and Im (σ_2) are plotted. Several features of Fig. 5(a) and (b) are noteworthy. First, we observe the excellent accuracy of the perturbation method derived in this paper. On the scale of the plot, our results and the "exact" results are virtually indistinguishable.

Second, all three calculated curves merge with increasing t_3 as the coupling ceases to be important. In this con-

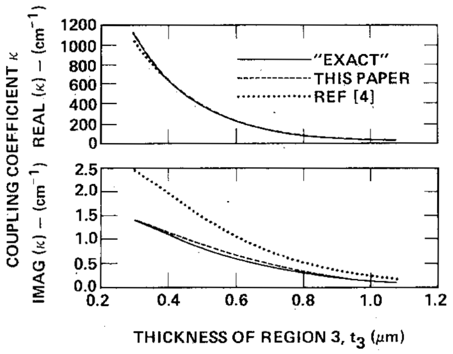

Fig. 6. Coupling coefficients versus thickness of region 3 for identical waveguides.

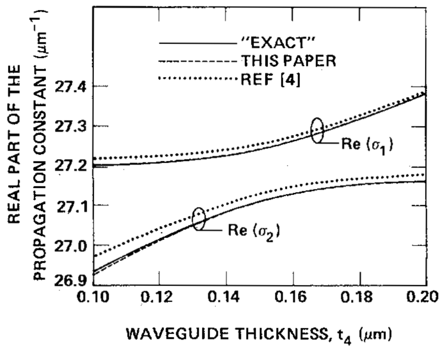

(a)

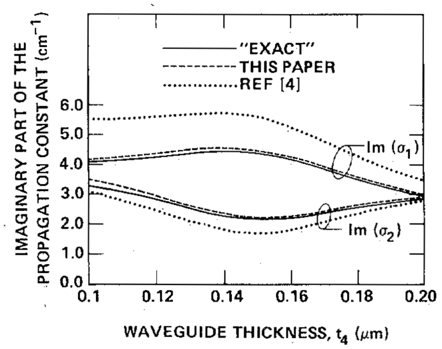

(b)

Fig. 7. (a)(b) Propagation constants versus waveguide thickness t_4. The waveguides are identical for $t_4 = 0.15$ μm.

nection it is also interesting to note that σ_1 and σ_2 approach each other with increasing t_3 as is to be expected. Third, as $t_3 \rightarrow 0$, the σ_2 mode becomes cut off at $t_3 \approx 0.0395$ μm (not shown in Fig. 5) and only one system mode propagates. Although we do not claim validity for any coupled mode formalism in that regime, our results predict that σ_2 is cut off at $t_3 \approx 0.11$ μm, whereas according to [4] no cutoff occurs. Thus even in this limit the new theory is at least qualitatively correct. With decreasing t_3, the Im (σ_1) also exhibits interesting behavior. Initially, as the individual guides are brought into closer proximity, the Im (σ_1) increases because a greater fraction of the modal power propagates in region 3, but as that region continues to shrink, the trend reverses since there are no modal losses whatsoever in the limit $t_3 = 0$. Results computed according to [4] do not display this decrease within the range of t_3 in Fig. 5(b). Moreover, in Fig. 5(b) the differences between Im (σ_1) and Im (σ_2) calculated according to the prior theory predict substantially greater relative attenuation of the modes than does the improved theory.

For the example treated above, the individual waveguides are identical. Consequently, the coupling coefficients are equal and may be determined approximately from the exact modal propagation constants according to (see Appendix F)

$$\kappa_{ab} = \kappa_{ba} = (\sigma_1 - \sigma_2)/2. \tag{17}$$

Fig. 6 displays the real and imaginary parts of the coupling coefficients computed according to (17) which are labeled "exact." Coefficients calculated from (4a) are plotted as dashed curves, and the curves shown dotted are $\bar{\kappa}_{ab}$ defined by (9a). Once again we note the excellent accuracy of the equations derived in this paper and the substantial discrepancy in the Im (κ) between the old and current formulations.

Before turning to other examples, it is worthwhile to reconsider the geometry of Fig. 4 and our approach. We not only considered waveguide "b" as a perturbation to ϵ_a and conversely, but also $\Delta n_c^2 = \text{Im}\,(n_3^2)$ was regarded as a perturbation to both ϵ_a and ϵ_b. That decomposition is not unique. As one alternative, suppose that the Im (n_3^2) were included in both ϵ_a and ϵ_b so that the perturbations were only the real indices n_4^2 and n_2^2 for $\Delta\epsilon_a$ and $\Delta\epsilon_b$, respectively. Then one must compute complex propagation constants and complex fields, which are to be employed in evaluating the integrals of this paper. Evidently, the approach we have utilized of incorporating the imaginary refractive indices in the perturbations is substantially simpler.

The above example treats only the geometry with two identical waveguides. To develop insight into other situations, we first fix $t_3 = 0.4$ μm and vary t_4, the waveguide thickness, between 0.1 μm and 0.2 μm. The real and imaginary parts of the propagation constants are plotted in Fig. 7(a) and (b). We observe again that the accuracy of the coupled mode theory is considerably increased by the inclusion of C_{ab} and C_{ba}. The general behavior illustrated in Fig. 7(a) and (b) is also noteworthy. When $t_4 = 0.15$ μm, waveguides "a" and "b" are identical; and the σ_1 mode is symmetrical and the σ_2 mode is antisymmetrical. With decreasing t_4, the σ_1 mode increasingly resides in waveguide "a" (see Fig. 2(a)) and Re (σ_1) approaches the propagation constant of waveguide "a" alone, which is 27.188 μm^{-1}. Simultaneously, the σ_2 mode approaches cutoff at $t_4 = 0.0298$ μm. With increasing t_4 above 0.15 μm, the σ_1 mode propagates primarily in waveguide "b"; its propagation constant asymptotically approaches $2\pi \times 3.6/0.8 = 28.274$ μm^{-1} and its loss vanishes. In the same limit Re $(\sigma_2) \approx 27.188$ μm^{-1} and the analysis of [16] may be employed to determine Im (σ_2).

Next, we compare κ_{ab} and κ_{ba} with $\bar{\kappa}_{ab}$ and $\bar{\kappa}_{ba}$. Unfortunately, exact results for κ_{ab} and κ_{ba} do not exist since these coefficients only appear in the coupled mode for-

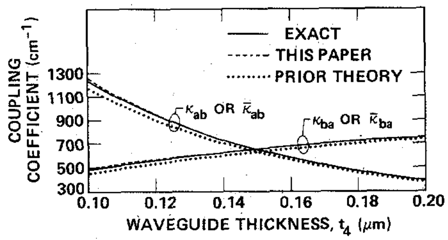

Fig. 8. Coupling coefficient versus waveguide thickness t_4 with $\mathrm{Im}(n_3^2) = 0$. The waveguides are identical for $t_4 = 0.15$ μm.

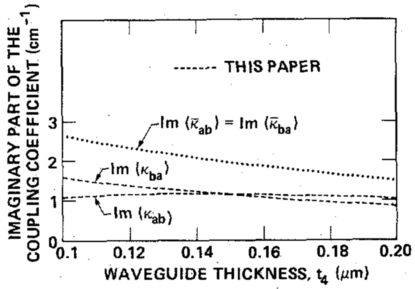

Fig. 9. Imaginary part of the coupling coefficient versus waveguide thickness t_4 with $\mathrm{Im}(n_3^2) = 1.299 \times 10^{-3}$. The waveguides are identical for $t_4 = 0.15$ μm.

malism. Nevertheless, numerical solutions for modes in the entire waveguide system may be utilized to estimate these quantities as described in Appendix F. Although the accuracy of these numerical values is indeterminate, for want of a better value we label them "exact." As shown in Appendix F, the evaluation of these "exact" coupling coefficients involves the calculation of the modal propagation constants, the modal patterns, and integrals thereof. All these steps are complicated for complex refractive indices, and so we limit our comparison exclusively to the real refractive index distribution of Fig. 4(a) with Im (n_3^2) set equal zero. Results are displayed in Fig. 8 for κ_{ab}, κ_{ba}, $\bar{\kappa}_{ab}$ and $\bar{\kappa}_{ba}$ as functions of the waveguide thickness t_4. Evidently, the expressions for κ_{ab} and κ_{ba} coincide more closely with the "exact" values, but as noted above, this coincidence is not a definitive test of accuracy.

With Im $(n_3^2) = i\,1.299 \times 10^{-3}$, real parts of all the coupling coefficients κ_{ab}, κ_{ba}, $\bar{\kappa}_{ab}$ and $\bar{\kappa}_{ba}$ are unchanged. Now, however, each of these quantities has the imaginary component plotted in Fig. (9). We observe that Im $(\bar{\kappa}_{ab})$ and Im $(\bar{\kappa}_{ba})$ appear identical and that is indeed the case as may be verified by comparing (9a) and (9b), since Im $(\Delta\epsilon_a) \equiv$ Im $(\Delta\epsilon_b)$. In contrast, Im (κ_{ab}) and Im (κ_{ba}) differ substantially because even though Im $(\tilde{\kappa}_{ab}) =$ Im $(\tilde{\kappa}_{ba})$ in (4a) and (4b), the other quantities in those equations are not the same. Moreover, the differences between Im (κ_{ab}) and Im (κ_{ba}) are quite important when these results are applied to phase array lasers, for example. Then the imaginary parts of the coupling coefficients are largely responsible for differences in the supermode thresholds.

To complete our study of varying the thickness t_4, we evaluated the coefficient of the $\sin^2 \psi z$ term in (16) with Im (n_3^2) set equal zero

$$\frac{\kappa_{ab}}{\psi^2}\,[\kappa_{ab} - \kappa_{ba} + \Delta(C_{ab} + C_{ba})]. \tag{18}$$

This expression is a measure of power conservation in our coupling formulation when power is being transferred from waveguide "b" to "a." That is, the power imbalance is proportional to the magnitude of (18) compared with unity. Clearly, for $t_4 = t_2 = 0.15$ μm, $\kappa_{ab} = \kappa_{ba}$ and $C_{ab} = C_{ba}$ so that (18) is identically zero. Over the range 0.1 μm $< t_4 <$ 0.2 μm, (18) attains a maximum value of 0.000326 for $t_4 = 0.1$ μm, which is illustrated in Fig. 1, and for practical purposes power is conserved to within 0.033 percent. In comparison, retaining only $|U|^2 + |V|^2$ in (11) and using $\bar{\kappa}_{ab}$ and $\bar{\kappa}_{ba}$ yields a power discrepancy of $\approx$20 percent in the form of the $\sin^2(\psi z)$ coefficient. We recall also that the small discrepancy of a nonzero value for (18) does not result from $|\kappa_{ab}| \neq |\kappa_{ba}|$, but rather from the last term in (11). In that connection when the waveguides are lossless, it follows from (18) being negligible that $\bar{\kappa}_{ab}$ approximates κ_{ab} and $\bar{\kappa}_{ba}$ approximates κ_{ba} although their defining equations are quite dissimilar. For the same geometry we compare $P^{(a)}$ and $P^{(b)}$ as given by (14) and (15), and find $(P^{(a)} - P^{(b)})/P^{(a)} = 0.00112$, thereby confirming that to within this numerical factor reciprocity is maintained. It is also interesting to observe that the difference between the field amplitudes calculated in connection with (14) and (15) is proportional to the expression $[\kappa_{ab} - \kappa_{ba} + \Delta(C_{ab} + C_{ba})]$ appearing in (18).

Results corresponding to those of Figs. 7–9 were calculated for the coupled waveguides with $t_3 = 0.4$ μm, $t_4 = 0.15$ μm and n_4 varied between 3.5 and 3.7. The behavior with changes in the relative waveguide strengths is quite similar to that described above in connection with Figs. 7–9 and the discussion applies in this case as well. The maximum value of (18) is 0.000511 which is attained for $n_4 = 3.5$, and in this geometry the prior theory with $\bar{\kappa}_{ab}$, $\bar{\kappa}_{ba}$ and only $|U|^2 + |V|^2$ produces a power discrepancy of $\approx$0.1 or $\approx$10 percent. For that case $(P^{(a)} - P^{(b)})/P^{(a)} = 0.0022$ when calculated from (14) and (15).

V. Conclusions

In conclusion, we have presented the derivation and results of a new coupled mode formulation for coupling between parallel waveguides. The formulation not only yields more accurate propagation constants, coupling coefficients, and array mode patterns than those employed heretofore, but it also has several other advantages. First, the results are completely general in that they are applicable to two parallel dielectric waveguides of arbitrary cross section, dissimilar index, and/or nonidentical shape. Second, it encompasses refractive index perturbations, which are not included in either waveguide, in an unambiguous manner. Third, the theory specializes in a simple manner to TE and TM modal cases. Fourth, we have shown that even in a lossless waveguide system the coupling coefficients κ_{ab} and κ_{ba} are not related by a complex conjugate relationship. Indeed, the magnitudes of κ_{ab} and κ_{ba} were shown to differ greatly in cases of dissimilar waveguide coupling without violating conservation of energy or reciprocity.

Appendix A
Orthogonality Relations

The following treatment is an extension of Kogelnik's approach [15] to include the case of waveguides with complex dielectric constant. For any two arbitrary electromagnetic fields which satisfy Maxwell's equations in some geometry

$$\nabla \cdot (\boldsymbol{E}_1 \times \boldsymbol{H}_2 - \boldsymbol{E}_2 \times \boldsymbol{H}_1) = 0. \tag{A1}$$

If the fields labeled "1" and "2" are two forward propagating modes of any waveguide geometry which is invariant in the axial z-direction, then

$$\boldsymbol{E}_1 = \boldsymbol{E}_\nu(x, y)\, e^{i\beta_\nu z} \tag{A2a}$$

$$\boldsymbol{E}_2 = \boldsymbol{E}_\mu(x, y)\, e^{i\beta_\mu z} \tag{A2b}$$

where β_m, $m = \nu, \mu$ are the complex propagation constants. After substituting in (A1) and invoking the divergence theorem [15], we obtain

$$\hat{z} \cdot \iint_{-\infty}^{\infty} (\boldsymbol{E}_{t_\nu} \times \boldsymbol{H}_{t_\mu} - \boldsymbol{E}_{t_\mu} \times \boldsymbol{H}_{t_\nu})\, dx\, dy = 0, \quad \text{for } \beta_\nu \neq \beta_{-\mu}. \tag{A3}$$

Repeating the above derivation using the backward traveling ν-mode $\boldsymbol{E}_1$

$$\boldsymbol{E}_1 = \boldsymbol{E}_{-\nu}(x, y)\, e^{-i\beta_\nu z} \tag{A4}$$

and the forward traveling μ-mode, $\boldsymbol{E}_2$, yields a relation similar to (A3) for $\beta_\mu \neq \beta_\nu$, except with $-\nu$ in place of ν. Applying now the z-reversal symmetry of Maxwell's equations [15] to the backward propagating mode, namely

$$\boldsymbol{E}_{t,-\nu}(x, y) = \boldsymbol{E}_{t,\nu}(x, y) \tag{A5a}$$

$$\boldsymbol{H}_{t,-\nu}(x, y) = -\boldsymbol{H}_{t,\nu}(x, y) \tag{A5b}$$

we find from (A3)

$$\hat{z} \cdot \iint_{-\infty}^{\infty} (\boldsymbol{E}_{t_\nu} \times \boldsymbol{H}_{t_\mu})\, dx\, dy = 0, \qquad \text{for } \beta_\nu \neq \pm\beta_\mu \tag{A6}$$

which is the desired orthogonality relation between two waveguide modes.

Appendix B
Mathematical Formulation

In this appendix we derive exact coupled wave equations satisfied by $U(z)$ and $V(z)$. The derivation is based on expanding the individual guided modes, written here as $\boldsymbol{E}_{t1}^{(a)}$ and $\boldsymbol{E}_{t1}^{(b)}$, and the overall field $\boldsymbol{E}_t$ in terms of the complete set of modes of the individual waveguides. Each individual waveguide supports guided plus radiation modes, which we consider to form a complete set for the representation of the other waveguide modes and the overall field. We have not proved that the expansion is valid mathematically, but the accuracy of our final results appears to justify the presumption of completeness.

Initially, then, we express any system fields in terms of the complete sets of individual waveguide modes

$$\boldsymbol{E}_t(x, y, z) = \sum_{\nu=1}^{\infty} a_\nu(z)\, \boldsymbol{E}_{t_\nu}^{(a)}(x, y) = \sum_{\nu=1}^{\infty} b_\nu(z)\, \boldsymbol{E}_{t_\nu}^{(b)}(x, y) \tag{B1a}$$

and

$$\boldsymbol{H}_t(x, y, z) = \sum_{\nu=1}^{\infty} a_\nu(z)\, \boldsymbol{H}_{t_\nu}^{(a)}(x, y) = \sum_{\nu=1}^{\infty} b_\nu(z)\, \boldsymbol{H}_{t_\nu}^{(b)}(x, y) \tag{B1b}$$

where the summations include integrations over the radiation modes. The coefficients in the expansions for the $\boldsymbol{E}_t$ and $\boldsymbol{H}_t$ fields are identical if we consider only fields propagating in the $+z$ half-space; neglecting backward waves introduces very small errors while substantially simplifying the derivation. The guided mode of each waveguide is now expressed as an expansion in the complete set of waveguide modes of the other guide, viz.,

$$\boldsymbol{E}_{t1}^{(b)}(x, y) = \sum_{\nu=1}^{\infty} C_\nu\, \boldsymbol{E}_{t_\nu}^{(a)}(x, y) \tag{B2a}$$

and

$$\boldsymbol{E}_{t1}^{(a)}(x, y) = \sum_{\nu=1}^{\infty} D_\nu\, \boldsymbol{E}_{t_\nu}^{(b)}(x, y) \tag{B2b}$$

where

$$C_\nu = 2\hat{z} \cdot \iint_{-\infty}^{\infty} [\boldsymbol{E}_{t1}^{(b)}(x, y) \times \boldsymbol{H}_{t_\nu}^{(a)}(x, y)]\, dx\, dy \tag{B3}$$

and (B3) defines D_ν when the superscripts "b" and "a" are interchanged. Identical expansions apply for $\boldsymbol{H}_{t1}^{(a)}$ and $\boldsymbol{H}_{t1}^{(b)}$. Upon substituting (B1a)–(B2b) in (1a) and solving for $\boldsymbol{E}_r$, we find

$$\begin{aligned}\boldsymbol{E}_r(x, y, z) &= [a_1(z) - U(z) - C_1 V(z)]\, \boldsymbol{E}_{t1}^{(a)}(x, y) + \sum_{\nu=2}^{\infty} [a_\nu(z) - C_\nu V(z)]\, \boldsymbol{E}_{t_\nu}^{(a)}(x, y) \\ &= [b_1(z) - V(z) - D_1 U(z)]\, \boldsymbol{E}_{t1}^{(b)}(x, y) + \sum_{\nu=2}^{\infty} [b_\nu(z) - D_\nu U(z)]\, \boldsymbol{E}_{t_\nu}^{(b)}(x, y)\end{aligned} \tag{B4}$$

and the same equation applies with $\boldsymbol{H}$ replacing $\boldsymbol{E}$ throughout.

Now by requiring that $\boldsymbol{E}_r$ (and $\boldsymbol{H}_r$) be orthogonal to the guided modes for all z, we obtain

$$a_1(z) = U(z) + C_1 V(z) \tag{B5a}$$

and

$$b_1(z) = D_1 U(z) + V(z). \tag{B5b}$$

The coefficients $a_\nu(z)$ satisfy the differential equations (see Appendix D).

$$\frac{da_\mu}{dz} = i\beta_\mu^{(a)} a_\mu + i \sum_{\nu=1}^{\infty} a_\nu \hat{\kappa}_{\nu\mu}^{(a)}, \qquad \mu = 1, 2, 3, \ldots \tag{B6}$$

and the $b_\nu(z)$ satisfy an analogous set for waveguide "b". The constants $\hat{\kappa}_{\nu\mu^{(m)}}$, $m = a, b$, relate the ν and μ modes of the *same* waveguide caused by the refractive index perturbation

$$\hat{\kappa}_{\nu\mu}^{(m)} = \omega \iint_{-\infty}^{\infty} \Delta\epsilon^{(m)}(x, y)\, \boldsymbol{E}_{t_\nu}^{(m)}(x, y) \cdot \boldsymbol{E}_{t_\mu}^{(m)}(x, y)\, dx\, dy - \iint_{-\infty}^{\infty} \frac{\epsilon^{(m)}(x, y)\, \Delta\epsilon^{(m)}(x, y)}{\epsilon_0\, n^2(x, y)} E_{z\nu}^{(m)}(x, y) \cdot E_{z\mu}^{(m)}(x, y)\, dx\, dy, \qquad m = a, b. \tag{B7}$$

Next for the purpose of deriving differential equations for $U(z)$ and $V(z)$, we substitute (B5a) and (B5b) in (B6) and its equivalent for $b_\mu(z)$, and find, after some manipulation

$$\frac{dU}{dz} + C_1 \frac{dV}{dz} = i\,[\beta_1^{(a)} + \hat{\kappa}_{11}^{(a)}]\, U + i\,[C_1\beta_1^{(a)} + \tilde{\kappa}_{ab}]V + i \sum_{\nu=2}^{\infty} \hat{\kappa}_{\nu 1}^{(a)}\, [a_\nu(z) - C_\nu V(z)] \tag{B8a}$$

$$\frac{dV}{dz} + D_1 \frac{dU}{dz} = i[\beta_1^{(b)} + \hat{\kappa}_{11}^{(b)}]\, V + i\,[D_1\beta_1^{(b)} + \tilde{\kappa}_{ba}]U + i \sum_{\nu=2}^{\infty} \hat{\kappa}_{\nu 1}^{(b)}\, [b_\nu(z) - D_\nu U(z)] \tag{B8b}$$

where

$$\tilde{\kappa}_{ab} = \omega \iint_{-\infty}^{\infty} \Delta\epsilon^{(a)}\, \boldsymbol{E}_{t_1}^{(a)} \cdot \boldsymbol{E}_{t_1}^{(b)}\, dx\, dy - \omega \iint_{-\infty}^{\infty} \frac{\epsilon^{(b)}\Delta\epsilon^{(a)}}{\epsilon_0 n^2} E_{z_1}^{(a)}\, E_{z_1}^{(b)}\, dx\, dy \tag{B9}$$

and $\tilde{\kappa}_{ba}$ is given by the same expression with (a) and (b) interchanged. In deriving (B9) contributions of radiation modes have been summed as shown in Appendix E. At this point we neglect the higher order terms in (B8a) and (B8b) and solve those equations simultaneously to obtain (2a) and (2b). In the body of the paper $\tilde{\kappa}_{aa} = \hat{\kappa}_{11}^{(a)}$, $\tilde{\kappa}_{bb} = \hat{\kappa}_{11}^{(b)}$, $C_{ab} = C_1$ and $C_{ba} = D_1$.

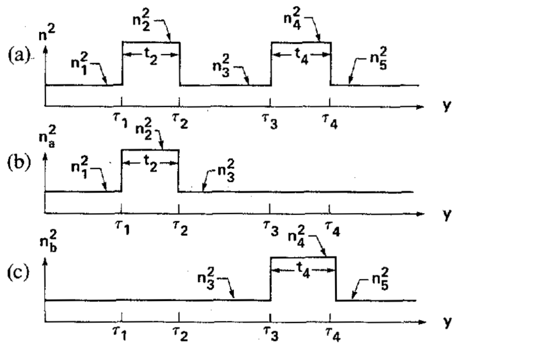

Fig. 10. Illustrating the decomposition of two parallel planar guides.

Appendix C
TE and TM Mode Coupling

Several dielectric waveguiding geometries may be treated exactly or approximately by utilizing TE and TM modes. These include slab waveguides, rectangular guides amenable to analysis by the equivalent index method (see [17, references] and also a discussion of stripe waveguides and their treatment by the effective index method in [15]), and circular weakly guiding structures. In the first two cases the refractive indexes n_a^2 and n_b^2 are illustrated in Fig. 10 and $n^2(x, y) \neq n_a^2(x, y) + n_b^2(x, y)$. The perturbations are $\Delta\epsilon^{(a)} = \epsilon_0 \Delta n_a^2 = \epsilon_0(n_4^2 - n_1^2)$ for $\tau_3 < y < \tau_4$ and $\Delta\epsilon^{(b)} = \epsilon_0 \Delta n_b^2 = \epsilon_0(n_2^2 - n_1^2)$ for $\tau_1 < y < \tau_2$. In the event n_1^2, n_3^2 and/or n_5^2 differ, a more complicated decomposition is needed; the optimum choice may not be clear. Moreover, if there were an additional index perturbation Δn_c^2 which was located in an interval denoted Y, then Δn_c^2 would be added to both Δn_a^2 and Δn_b^2 in that interval.

For the TE modes, only E_x is nonzero and we employ the scalars $E_1^{(a)}$ and $E_1^{(b)}$. Once $E_1^{(m)}$, $m = a, b$ is determined by solving the scalar wave equation [4], [10], [15], we have

$$C_{pq} = \frac{2\beta_1^{(p)}}{\omega\mu_0} \int_{-\infty}^{\infty} E_1^{(p)}\, E_1^{(q)}\, dy, \qquad p, q = a, b \tag{C1}$$

and the modes are normalized such that $C_{aa} = C_{bb} = 1$. The propagation constant corrections are

$$\tilde{\kappa}_{aa} = \omega\epsilon_0\, (n_4^2 - n_1^2) \int_{\tau_3}^{\tau_4} [E_1^{(a)}]^2\, dy \tag{C2a}$$

and

$$\tilde{\kappa}_{bb} = \omega\epsilon_0\, (n_2^2 - n_1^2) \int_{\tau_1}^{\tau_2} [E_1^{(b)}]\, dy \tag{C2b}$$

and the quantities $\tilde{\kappa}_{ab}$ and $\tilde{\kappa}_{ba}$ are given by

$$\tilde{\kappa}_{ab} = \omega\epsilon_0\, (n_4^2 - n_1^2) \int_{\tau_3}^{\tau_4} [E_1^{(a)}\, E_1^{(b)}]\, dy \tag{C3a}$$

and

$$\tilde{\kappa}_{ba} = \omega\epsilon_0 (n_2^2 - n_1^2) \int_{T1}^{T2} [E_1^{(a)} E_1^{(b)}]. \tag{C3b}$$

Were there an additional index perturbation Δn_c^2 in Y, (C2a)–(C3b) would each contain an additional integral over the interval Y.

For TM modes only H_x is non-zero and is written $H_1^{(m)}$, $m = a, b$. Upon solving for $H_1^{(m)}$, we obtain

$$C_{pq} = \frac{2\beta_1^{(q)}}{\omega\epsilon_0} \int_{-\infty}^{\infty} \frac{H_1^{(p)} H_1^{(q)}}{n_q^2} \, dy, \qquad p, q = a, b \tag{C4}$$

and the fields are normalized such that $C_{aa} = C_{bb} = 1$. Now in the TM case,

$$\tilde{\kappa}_{aa} = \frac{(n_4^2 - n_1^2)}{\omega\epsilon_0 n_1^2} \int_{T3}^{T4} \left\{ \frac{[\beta_1^{(a)}]^2}{n_1^2} [H_1^{(a)}(y)]^2 + \frac{1}{n_4^2} \left[\frac{\partial H_1^{(a)}(y)}{\partial y} \right]^2 \right\} dy \tag{C5a}$$

and

$$\tilde{\kappa}_{bb} = \frac{(n_2^2 - n_1^2)}{\omega\epsilon_0 n_1^2} \int_{T1}^{T2} \left\{ \frac{[\beta_1^{(b)}]^2}{n_1^2} [H_1^{(b)}(y)]^2 + \frac{1}{n_2^2} \left[\frac{\partial H_1^{(b)}(y)}{\partial y} \right]^2 \right\} dy \tag{C5b}$$

whereas

$$\tilde{\kappa}_{ab} = \frac{(n_4^2 - n_1^2)}{\omega\epsilon_0 n_4^2 n_1^2} \int_{T3}^{T4} \left\{ \beta_1^{(a)} \beta_1^{(b)} H_1^{(a)} H^{(b)} + \frac{\partial H_1^{(a)}}{\partial y} \frac{\partial H_1^{(b)}}{\partial y} \right\} dy \tag{C6a}$$

and

$$\tilde{\kappa}_{ba} = \frac{(n_2^2 - n_1^2)}{\omega\epsilon_0 n_2^2 n_1^2} \int_{T1}^{T2} \left\{ \beta_1^{(a)} \beta_1^{(b)} H_1^{(a)} H_1^{(b)} + \frac{\partial H_1^{(a)}}{\partial y} \frac{\partial H_1^{(b)}}{\partial y} \right\} dy. \tag{C6b}$$

Appendix D
Derivation of (B6) and (B7)

The following treatment is for a single waveguide with perturbations. The derivation of [15] is modified to include complex dielectric constants. The polarization vector is separated into two parts, $\epsilon \boldsymbol{E} + \boldsymbol{P}$ where $\boldsymbol{P}$ represents excitation sources and an external pertubation polarization. From Maxwell's equations, for any two arbitrary electromagnetic fields

$$\nabla \cdot (\boldsymbol{E}_2 \times \boldsymbol{H}_1 - \boldsymbol{E}_1 \times \boldsymbol{H}_2) = i\omega (\boldsymbol{E}_2 \cdot \boldsymbol{P}_1 - \boldsymbol{E}_1 \cdot \boldsymbol{P}_2). \tag{D1}$$

which reduces to (A1) when $\boldsymbol{P}_1 \equiv \boldsymbol{P}_2 \equiv 0$. However, $\boldsymbol{P}_2(x, y, z) = 0$ if we assume that $\{\boldsymbol{E}_2, \boldsymbol{H}_2\}$ is a mode of the unperturbed waveguide. Then integration of (D1) over the cross section and invoking the divergence theorem yields

$$\hat{z} \cdot \iint_{-\infty}^{\infty} \frac{\partial}{\partial z} (\boldsymbol{E}_2 \times \boldsymbol{H}_1 - \boldsymbol{E}_1 \times \boldsymbol{H}_2) \, dx \, dy = i\omega \iint_{-\infty}^{\infty} (\boldsymbol{E}_2 \cdot \boldsymbol{P}_1) \, dx \, dy \tag{D2}$$

where the line integral vanishes [15]. Next the transverse components of the perturbed field $\{\boldsymbol{E}_1, \boldsymbol{H}_1\}$ are expanded in the complet set of unperturbed modes of the waveguide:

$$\boldsymbol{E}_{1_t}(x, y, z) = \sum_{\nu=1}^{\infty} [p_\nu(z) + q_\nu(z)] \, \boldsymbol{E}_{t_\nu}(x, y) \tag{D3a}$$

$$\boldsymbol{H}_{1_t}(x, y, z) = \sum_{\nu=1}^{\infty} [p_\nu(z) - q_\nu(z)] \, \boldsymbol{H}_{t_\nu}(x, y) \tag{D3b}$$

where $p_\nu(z)$ and $q_\nu(z)$ represent forward and backward waves. Now if $\{\boldsymbol{E}_2, \boldsymbol{H}_2\}$ is a mode with propagation consant β_μ, then

$$\boldsymbol{E}_2(x, y, z) = \boldsymbol{E}_{\pm\mu}(x, y) \, e^{\pm i\beta_\mu z} \tag{D4}$$

where the upper and lower signs correspond to propagation in the $\pm z$ direction. Upon substituting (D3a)–(D4) in (D2) and invoking (A5a) and (A5b) together with the equation for $\boldsymbol{H}_2$, we obtain

$$\frac{dp_\mu}{dz} - i\beta_\mu p_\mu = i\omega R_{-\mu}, \qquad \mu = 1, 2, 3 \cdots \tag{D5a}$$

and

$$\frac{dq_\mu}{dz} + i\beta_\mu q_\mu = -i\omega R_\mu, \qquad \mu = 1, 2, 3, \cdots \tag{D5b}$$

where

$$R_\mu = \iint_{-\infty}^{\infty} \boldsymbol{E}_\mu(x, y) \cdot \boldsymbol{P}_1(x, y, z) \, dx \, dy. \tag{D6}$$

Next we evaluate $\boldsymbol{P}_1 = \Delta\epsilon \boldsymbol{E}_1$, to obtain

$$\boldsymbol{P}_1 = \Delta\epsilon \sum_{\nu=1}^{\infty} \left\{ [p_\nu(z) + q_\nu(z)] \boldsymbol{E}_{t_\nu} + \frac{\epsilon}{\epsilon + \Delta\epsilon} [p_\nu(z) - q_\nu(z)] \, \hat{z} E_{z_\nu} \right\}. \tag{D7}$$

Finally, employing the expression for $\boldsymbol{P}_1$ in the definition of R_μ, yields

$$\frac{dp_\mu}{dz} - i\beta_\mu p_\mu = i\omega (S_\mu - T_\mu), \qquad \mu = 1, 2, 3, \cdots \tag{D8a}$$

and

$$\frac{dq_\mu}{dz} + i\beta_\mu q_\mu = -i\omega (S_\mu + T_\mu), \qquad \mu = 1, 2, 3, \cdots \tag{D8b}$$

where

$$S_\mu = \sum_{\nu=1}^{\infty} (p_\nu + q_\nu) \iint_{-\infty}^{\infty} \Delta\epsilon \boldsymbol{E}_{t_\mu} \cdot \boldsymbol{E}_{t_\nu}\, dx\, dy \tag{D9a}$$

and

$$T_\mu = \sum_{\nu=1}^{\infty} (p_\nu - q_\nu) \iint_{-\infty}^{\infty} \frac{\epsilon\, \Delta\epsilon}{\epsilon + \Delta\epsilon} E_{z_\mu} E_{z_\nu}\, dx\, dy. \tag{D9b}$$

In deriving these results, the relationship $E_{z,-\nu} = -E_{z,\nu}$ has been employed. The results differ from those of [15] in that the fields are not complex conjugates and the integrations over $E_{z,\nu}$ are reversed in sign. For real dielectric constants, the results coincide with those of [15].

Assuming now that waveguide "a" is the unperturbed waveguide, and that waveguide "b" acts to perturb waveguide "a," we replace $p_\nu(z)$ by $a_\nu(z)$ and set $q_\nu(z) = 0$ (since the backward waves do not grow significantly if they are initially unexcited). Then (D8a) reduces to (B6) and the integrals in (D9a) and (D9b) are identifiable as the coefficients $\hat{\kappa}_{\nu\mu}^{(a)}$ as in (B7).

Appendix E
Derivation of (B8a)–(B9)

By substituting (B5a) in (B6) we obtain

$$\frac{dU}{dz} + C_1 \frac{dV}{dz} = i\,[\beta_1^{(a)} + \hat{\kappa}_{11}^{(a)}]\,(V + C_1 V) + i \sum_{\nu=2}^{\infty} a_\nu(z)\, \hat{\kappa}_{\nu 1}^{(a)}. \tag{E1}$$

Next, by including $(\Sigma_{\nu=2}^{\infty} C_\nu \hat{\kappa}_{\nu 1}^{(a)})V(z)$ in (E1), we obtain (B8a) with

$$\tilde{\kappa}_{ab} = \sum_{\nu=1}^{\infty} C_\nu \hat{\kappa}_{\nu 1}^{(a)} \tag{E2}$$

expressed in the form of an infinite series, where C_ν and $\hat{\kappa}_{\nu 1}^{(a)}$ are simple integrals as defined in (B3) and (B7), respectively. Our goal is to obtain a more convenient expression for $\tilde{\kappa}_{ab}$ that can be calculated in a straightforward manner. Upon substituting (B7) into (E2) and interchanging the order of summation and integration, we find that

$$\tilde{\kappa}_{ab} = \omega \iint_{-\infty}^{\infty} \Delta\epsilon^{(a)}(x, y) \left[\sum_{\nu=1}^{\infty} C_\nu \boldsymbol{E}_{t\nu}^{(a)}(x, y)\right] \cdot \boldsymbol{E}_{t_1}^{(a)}(x, y)\, dx\, dy - \omega \iint_{-\infty}^{\infty} \frac{\Delta\epsilon^{(a)}(x, y)}{\epsilon_0 n^2(x, y)} \left[\epsilon^{(a)}(x, y) \sum_{\nu=1}^{\infty} C_\nu E_{z\nu}^{(a)}(x, y)\right] \cdot E_{z_1}^{(a)}(x, y)\, dx\, dy. \tag{E3}$$

The first summation in (E3) is given by (B2a). The second summation is evaluated using Maxwell's equations and the $\boldsymbol{H}$-field expansion analogous to (B2a), i.e.,

$$\epsilon^{(b)} E_{z_1}^{(b)} = (i/\omega)\, \nabla_t \times \sum_{\nu=1}^{\infty} C_\nu \boldsymbol{H}_{t_\nu}^{(a)} = \epsilon^{(a)} \sum_{\nu=1}^{\infty} C_\nu\, E_{z_\nu}^{(a)}. \tag{E4}$$

Thus we derive (B9).

Appendix F
Definition of Coupling Coefficients in Terms of System Modes

Assuming that $\{\boldsymbol{E}_t(x, y, z), \boldsymbol{H}_t(x, y, z)\}$ in (1a) and (1b) are the transverse components of either one of the two guided array modes (i.e., an exact "supermode") we have

$$\boldsymbol{E}_t(x, y, z) = \boldsymbol{E}_t^{(m)}(x, y) e^{i\sigma_m z}, \qquad m = 1, 2 \tag{F1a}$$

$$\boldsymbol{H}_t(x, y, z) = \boldsymbol{H}_t^{(m)}(x, y) e^{i\sigma_m z}, \qquad m = 1, 2. \tag{F1b}$$

Substituting (F1a) into (1a), multiplying by $\boldsymbol{H}_{t_1}^{(n)}(x, y)$ $n = a, b$ and integrating over the entire cross section at some value of z, we obtain:

$$u_m + C_{ab} v_m = I_{ma}, \qquad m = 1, 2 \tag{F2a}$$

and

$$C_{ba} u_m + v_m = I_{mb}, \qquad m = 1, 2 \tag{F2b}$$

where

$$I_{mn} = 2\hat{z} \cdot \iint_{-\infty}^{\infty} [\boldsymbol{E}_t^{(m)}(x, y) \times \boldsymbol{H}_{t_1}^{(n)}(x, y)]\, dx\, dy, \quad m = 1, 2, \quad n = a, b. \tag{F3}$$

In deriving these results, the definitions of C_{ab} and C_{ba} and the orthogonality of $\boldsymbol{E}_r$ to the guided modes of the individual waveguides were employed.

Solving now the set of four equations (F2a), (F2b) for u_m, v_m, $m = 1, 2$, we obtain

$$v_m = (I_{mb} - C_{ba} I_{ma})/(1 - C_{ab} C_{ba}), \qquad m = 1, 2 \tag{F4a}$$

and

$$u_m = (I_{ma} - C_{ab}\, I_{mb})/(1 - C_{ab} C_{ba}), \qquad m = 1, 2. \tag{F4b}$$

When (F4a) and (F4b) are substituted in (2a) and (2b), we obtain

$$\sigma_m u_m = \gamma^{(a)} u_m + \kappa_{ab} v_m, \qquad m = 1, 2 \tag{F5a}$$

and

$$\sigma_m v_m = \gamma^{(b)} v_m + \kappa_{ba} u_m, \qquad m = 1, 2 \tag{F5b}$$

upon requiring that the equations be satisfied for all z. The resulting four equations are then solved numerically for $\gamma^{(a)}$, $\gamma^{(b)}$, κ_{ab} and κ_{ba}, i.e.,

$$\begin{bmatrix} u_1 & v_1 & 0 & 0 \\ 0 & 0 & u_1 & v_1 \\ u_2 & v_2 & 0 & 0 \\ 0 & 0 & u_2 & v_2 \end{bmatrix} \begin{bmatrix} \gamma^{(a)} \\ \kappa_{ab} \\ \kappa_{ba} \\ \gamma^{(b)} \end{bmatrix} = \begin{bmatrix} \sigma_1 u_1 \\ \sigma_1 v_1 \\ \sigma_2 u_2 \\ \sigma_2 v_2 \end{bmatrix}. \tag{F6}$$

For two identical waveguides, the solutions become

$$\kappa_{ab} = \kappa_{ba} = (\sigma_1 - \sigma_2)/2 \tag{F7}$$

and

$$\gamma^{(a)} = \gamma^{(b)} = (\sigma_1 + \sigma_2)/2. \tag{F8}$$

Acknowledgment

The authors thank Dr. R. V. Schmidt, Dr. P. S. Cross, Dr. E. A. J. Marcatili, and Dr. H. Kogelnik for helpful discussions.

References

[1] E. A. J. Marcatili, "Dielectric rectangular waveguide and directional coupler for integrated optics," *Bell Syst. Tech. J.*, vol. 48, pp. 2071–2102, 1969.
[2] D. Marcuse, "The coupling of degenerate modes in two parallel dielectric waveguides," *Bell Syst. Tech. J.*, vol. 50, pp. 1791–1816, 1971.
[3] H. Kogelnik and R. V. Schmidt, "Switched directional couplers with alternating $\Delta\beta$," *IEEE J. Quantum Electron.*, vol. QE-12, pp. 396–401, 1976.
[4] H. F. Taylor and A. Yariv, "Guided wave optics," *Proc. IEEE*, vol. 62, pp. 1044–1060, 1974.
[5] D. R. Scifres, W. Streifer, and R. D. Burnham, "High-power coupled-multiple-stripe phase-locked injection laser," *Appl. Phys. Lett.*, vol. 34, pp. 259–261, 1979.
[6] D. E. Ackley and R. W. H. Engelmann, "Twin-stripe injection laser with leak-mode coupling," *Appl. Phys. Lett.*, vol. 37, pp. 866–868, 1981.
[7] J. Katz, E. Kapon, C. Lindsey, S. Margalit, and A. Yariv, "Far-field distributions of semi-conductor phase-locked arrays with mutliple contacts," *Elect. Lett.*, vol. 19, pp. 660–662, 1983.
[8] J. K. Butler, D. E. Ackley, and D. Botez, "Coupled mode analysis of phased-locked injection laser arrays," *Appl. Phys. Lett.*, vol. 44, pp. 293–295, 1984; also in *Tech. Dig Conf. Optical Fiber Communication* (New Orleans, LA), pp. 44–46, Jan. 1984.
[9] J. P. van der Ziel, H. Temkin, R. A. Logan, and R. D. Dupuis, "High-power picosecond pulse generation in GaAs multiquantum well phased-locked laser arrays using pulsed current injection," *IEEE J. Quantum Electron.*, vol. QE-20, pp. 1236–1242, 1984, and references therein.
[10] D. Marcuse, *Light Transmission Optics*. New York: Van Nostrand, 1972.
[11] A. Yariv, "Coupled mode theory for guided-wave optics," *IEEE J. Quantum Electron.*, vol. QE-9, pp. 919–933, 1973.
[12] Y. Suematsu and K. Kishino, "Coupling coefficients in strongly coupled dielecric waveguides," *Radio Sci.*, vol. 12, pp. 587–592, 1977.
[13] E. Marom, O. G. Ramer, and S. Ruschin, "Relation between normal mode and coupled mode analyses of parallel waveguides," *IEEE J. Quant. Electron.*, QE-20, pp. 1311–1319, 1984.
[14] A. W. Snyder and J. D. Love, *Optical Waveguide Theory*. London and New York: Chapman and Hall, 1983, pp. 570 and following.
[15] H. Kogelnik, "Theory of dielectric waveguides" in *Integrated Optics*, T. Tamir, Ed. New York: Springer-Verlag, 1975, ch. 2.
[16] W. Streifer, R. D. Burnham, and D. R. Scifres, "Substrate radiation losses in GaAs heterostructure lasers," *IEEE J. Quant. Electron.*, vol. QE-12, pp. 177–182, 1976.
[17] G. B. Hocker and W. K. Burns, "Mode dispersion in diffused channel waveguides by the effective index method," *Appl. Opt.*, vol. 16, pp. 113–118, 1977.

*

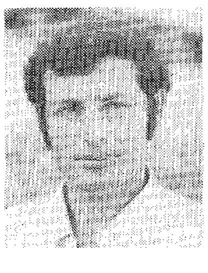

Amos Hardy (SM'85) was born in Hungary on February 9, 1942 and emigrated to Israel in 1948. He received the B.Sc. and M.Sc. degrees from the Hebrew University of Jerusalem, Jerusalem, Israel, and the Ph.D. degree in applied physics from the Weizmann Institute of Science, Rehovot, Israel in 1966, 1969, and 1975, respectively.

From 1975 to 1983 he was with the Department of Electronics, Weizmann Institute of Science. From 1976 to 1979 he was on leave and worked at Stanford University, Stanford, CA, on various laser resonator problems, optical phase conjugation, and optical rotation sensing systems. During the summer of 1982, he was a Visiting Scientist at Bell Laboratories, Holmdel, NJ, where he worked on problems related to DFB lasers. Since 1983 he has been with the Faculty of Engineering at the Tel Aviv University. From June 1984 to July 1985, he was a Visiting Scientist at Xerox Palo Alto Research Center where he was engaged in the analysis of phase-coupled laser arrays. During the summer of 1985 he was a Visiting Associate Professor at the University of New Mexico. His research interest involves analysis of dye laser systems, DFB lasers, diode lasers, optical resonators and waveguides, propagation of laser beams, optical phase conjugation, and the study of optical systems for inertial rotation sensing.

While at the Weizmann Institute, Dr. Hardy held the Ruth E. Recu Career Development Chair. He is a member of the Optical Society of America.

*

William Streifer (S'56–M'58–SM'74–F'79) was graduated from the Bronx High School of Science in 1953. He received the B.E.E. degree (magna cum laude) from the City College of New York in 1957, the M.S. degree in electrical engineering from Columbia University, New York, NY, in 1959, and the Ph.D. degree from Brown University, Providence, RI, in 1962.

From 1957 to 1959, he was a Lecturer in the Department of Electrical Engineering, City College of New York. From 1958 to 1959, he was a Research Engineer at the Heat and Mass Flow Analyzer Laboratory, Columbia University. At Brown University, from 1959 to 1961, he was a National Science Foundation Fellow. He taught in the Division of Engineering and later held a Bell Telephone Laboratories fellowship. From 1962 to 1972, he was successively Assistant Professor, Associate Professor, and Professor of Electrical Engineering at the University of Rochester. During the academic year 1969–1970, he was a Visiting Associate Professor at Stanford University. In 1972, he joined the Xerox Palo Alto Research Center as a Principal Scientist. Thereafter, he held the positions of Research Fellow and Senior Research Fellow. During 1976–1979, he introduced and taught a graduate course, "Integrated and Fiber Optics", at Stanford University. For one month during 1982, he was Einstein Fellow at the Weizmann Institute, Rehovat, Israel, and in July 1984, he was a Visiting Fellow at the Institute for Advanced Study, Australian National University. In 1985 he was appointed Director, Center for High Technology Materials, and Professor of Electrical Engineering at the University of New Mexico.

Dr. Streifer has authored or coauthored over one hundred fifty papers and forty patents. In addition to work published in the open literature, he has carried out many consulting and research tasks of a confidential nature for Xerox Corporation. He has also been Chairman, Council of Research Fellows, at Xerox Corporation. He is a Fellow of the Optical Society of America, the Editor of the *IEEE Journal of Quantum Electronics*, and has been Associate Editor of that publication as well as the *Journal of the Optical Society* and the *Journal of Optical Communications*. He served on the Editorial Board of the *IEEE Transactions on Microwave Theory and Techniques*. As a member of the Quantum Electronics and Applications Society Administrative Commitee, he organized the local sections, held the office of Treasurer, and served on the Education Subcommittee. He was Technical Program Chairman of the Eighth International Semiconductor Laser Conference and has served both the IEEE and Optical Society of America in several other capacities. He is a member of Sigma Xi, Eta Kappa Nu, Tau Beta Pi, and the U.S. National Committee of the International Commission for Optics. He was appointed to the IEEE University Accreditation Committee, and has also assisted the National Science Foundation, the U.S. Congress, Office of Technology Assessment, and the U.S. Air Force. He is listed in *Who's Who*, *American Men and Women of Science*, *Engineers of Distinction*, and several other volumes. He received the IEEE Centennial Service Medal in 1984 and the IEEE Jack Morton Medal in 1985.